Available online at www.sciencedirect.com
ScienceDirect
Engineering Fracture Mechanics 74 (2007) 273–289
Engineering Fracture Mechanics
www.elsevier.com/locate/engfracmech

Structural damage diagnosis and life-time assessment by acoustic emission monitoring

A. Carpinteri *, G. Lacidogna, N. Pugno

Department of Structural Engineering and Geotechnics, Politecnico di Torino, Corso Duca Degli Abruzzi 24, 10129 Torino, Italy

Available online 20 March 2006

Abstract

The acoustic emission technique is applied to identify defects and damage in reinforced concrete structures and masonry buildings. By means of this technique, a particular methodology has been put forward for crack propagation monitoring and damage assessment, in structural elements under service conditions. This technique permits to estimate the amount of energy released during fracture propagation and to obtain information on the criticality of the ongoing process. In addition, based on fracture mechanics concepts, a fractal or multiscale methodology is proposed to predict the damage evolution and the time to structural collapse.

Keywords: Acoustic emission monitoring; Structural assessment; Damage mechanics; Crack growth; Life prediction

1. Introduction

The evaluation of safety and reliability for reinforced concrete structures, like bridges and viaducts or masonry historical buildings, represents a complex task at the cutting edge of technological research. Due to these reasons, the diagnosis and monitoring techniques are assuming an increasing importance in the evaluation of structural conditions and reliability. Among these methods, the non-destructive methodology based on acoustic emission (AE) proves to be very effective [1].

This method of damage detection, that now is attracting considerable attention, was employed at the beginning of the 1960s for the inspection of pressure vessels in USA. After this starting stage, the level of research interest became so high that international AE congresses were held all over the World. In response to this high level of research activity, AE has been investigated increasingly as a diagnostic tool for existing concrete structures [2].

Earlier in the history of AE, major efforts were directed to probing the fundamentals of AE phenomena and their behavior during deformation and fracture of metallic materials. It started in Germany with the research work on metals carried out by Kaiser [3], although AE on rock was already known in mining technology. With

* Corresponding author. Tel.: +39 011 564 4850; fax: +39 011 564 4899.
E-mail address: alberto.carpinteri@polito.it (A. Carpinteri).

0013-7944/$ - see front matter
doi:10.1016/j.engfracmech.2006.01.036

regard to the basis of AE research in concrete, the early scientific papers were published in the 1960s. Particularly interesting are the contributions by Rüsch [4], L'Hermite [5] and Robinson [6]. They discussed the relation between fracture process and volumetric change in the concrete under uniaxial compression. The most important applications of AE to structural concrete elements started in the late 1970s, when the original technology developed for metals was modified to suit heterogeneous materials [7,8]. At present, the AE technique is sometimes applied to concrete or reinforced concrete structures.

Another main field for AE research is actually the signal source location. This methodology is applied in order to determine the defects position and their orientation in the material. Among the first researchers who studied this methodology we find Shah and Li [9]. They applied the AE source location to identify the fracture process zone for cementitious materials, mainly subject to strain-softening loads. In this field, Ohtsu [2] carried out further studies, again performed at the laboratory scale. This studies concern the AE source location in bending tests of reinforced concrete beams. Two failure modes, bending failure and diagonal shear failure, are clearly identified from 3-D maps of source location.

Some later applications of AE technique to construction monitoring are described in Carpinteri and Lacidogna [10–12] where the AE monitoring is applied to forecast the damage evolution in reinforced concrete and in historical masonry buildings. In these papers, the stability evaluation of the structures is performed connecting the damage evolution, estimable by the dating and systematic survey, with the cumulative distribution of AE events in time. Since cracking is a multiscale phenomenon, recently AE data have been interpreted by statistical and fractal theories [13] like that proposed by Carpinteri and Pugno [14–16] for fragmentation and comminution phenomena.

2. Fundamentals of AE technique

Acoustic emission is represented by the class of phenomena whereby transient elastic waves are generated by the rapid release of energy from localized sources within a material. All materials produce AE during both the generation and propagation of cracks. The elastic waves move through the solid surface, where they are detected by sensors. These sensors are transducers that convert the mechanical waves into electrical signals. In this way, information about the existence and location of possible damage sources is obtained. This is similar to seismicity, where seismic waves reach the station placed on the earth surface [17,18]. Therefore, among the structural non-destructive tests, the AE monitoring technique is the only one able to detect a damage process at the same time when it occurs.

The AE method, which is called Ring-Down Counting or Event-Counting, considers the number of waves beyond a certain threshold level (measured in Volt) and is widely used for defect analysis [19,20]. As a first approximation, in fact, the cumulative number of counts N can be compared with the amount of energy released during the loading process, assuming that both quantities increase with the extent of damage (Fig. 1).

By means of this technique, we have analysed the evolution of cracks and estimated the released strain energy during their propagation in structural members. In particular, masonry historical buildings and reinforced concrete structures have been investigated.

3. Damage diagnosis of masonry buildings

Two masonry buildings have been monitored. The first one, called "Casa Capello" (Fig. 2), is located in the historical area of Rivoli, and was constructed upon pre-existing ruins, dating back to the XIV Century. This building has recently been object of complex interventions of functional extension and restoration. The AE methodology has been applied on certain walls of the building, in order to evaluate the status of the cracks that spread out after the collapse of a breast-wall [10]. In particular, the monitoring has involved two cracks which appeared inside the internal surface of the sustaining structure, at the ground floor level. Crack no. 1, monitored for about 900 h, has developed on a masonry wall reinforced with an external concrete surface. Crack no. 2 has been identified in a part of a wall, entirely built by bricks, and monitored for about 800 h.

Two transducers have been used to detect the AE released by the cracks. They were applied approximately 3 cm far from the top of cracks, to minimize signal attenuation. The dates of the first application of the transducers and their final removal, for the crack no. 1, are represented in Fig. 3. The graph, obtained by the mon-

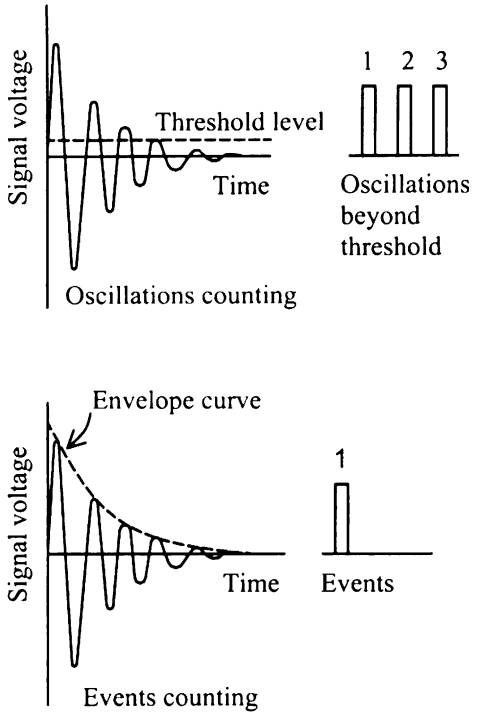

Fig. 1. Detected signals by AE technique.

Fig. 2. "Casa Capello" in Rivoli. On the background the bell tower of the Collegiata, on the foreground the breast wall that collapsed during the restoration works.

itoring data, describes how the behavior of the countings is proportional to the advancement of the cracks and the exhaustion of the ring-down counting clearly reveals the arrest of the cracks advancement.

Furthermore diagrams remark that the maximum counting of AE happens during the highest velocity of the crack advancement process. After this event, both counting and crack advancement tend to decrease rapidly, up to complete vanishing. We can therefore assume that the peak data of AE distribution do correspond

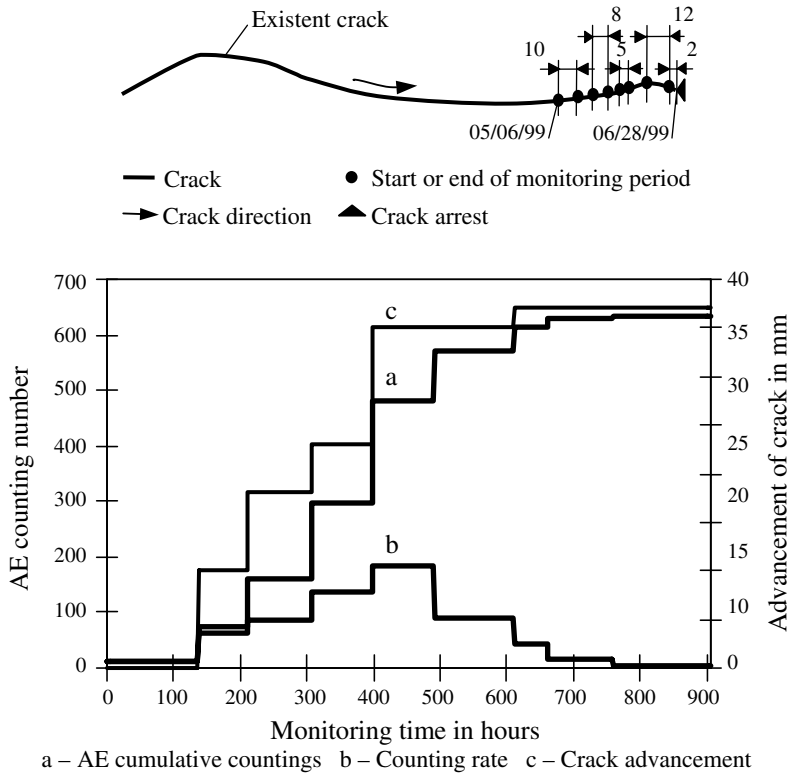

Fig. 3. Crack no. 1. development and AE monitoring results.

to the most critical period of advancement of the crack, which then reaches a condition of stability, proceeding towards the compressed zones of masonry. Diagrams related to time-advancing cracks show a stable behavior, as well as the diagrams that relate time to cumulative AE counting.

The second masonry building, called ''Torre Sineo'', dated XIII Century, is the tallest and most mighty of the medieval towers preserved in the town of Alba (Fig. 4). The structure squared planned, with size measured in 5.9×5.9 m, is approximately 39 meter high and is leaning to the northern side. The foundations lie below 3.5 m from the surface of the street level. The walls are variably thick between 0.8 and 2.0 m. The sustaining wall is ''a sacco'' with the external bricks joined with one centimeter thick mortar. The internal filling is composed by remainders of bricks tied using a poor mortar. The tower is incorporated for 15 m within a later dated building. Regarding the incorporated part, the floors have been realized through masonry vaults, while in the upper part of the tower the floors are made with wooden structures (Fig. 5).

The cracking network can be observed both on the internal and external masonry surfaces. The most significant cracks are inside the tower, mainly located between the 6th and 8th floors. On the external side we can observed minor cracks, mainly near the windows, more specifically between the 6th and 7th floors.

Through the AE monitoring, two cracks have been detected on the internal surface of the masonry at the 7th floor (Fig. 5): one located by a window, and the other nearby. The monitoring has reported a continuous damage process, characterized by a slow spread of cracks inside the brick walls. In the most damaged zone, we detected an arrest of the cracking process, since the cracks had achieved a new condition of stability in the compressed zones of masonry.

In this particular case, it could be observed how any appreciable crack advancement, in the monitored zone, is often correlated to a seismic event. In the diagram of Fig. 6, we have overlapped the cumulative AE function of the monitored area with the seismic occurrences and their intensity, happened in Alba region in the same period of time. The seismic events data were provided by the National Institute for Geophysics and Volcanology in Rome. This detection might prove how the tower behavior is stable when it is only subject

Fig. 4. Sineo Tower in Alba.

to vertical loads. The structure, in fact, does not have the capacity to respond elastically when it is subject to horizontal or shaking actions.

4. Damage diagnosis of concrete frames

The AE methodology was applied to two buildings, with reinforced concrete structure [21]. The first building, located in the city of Moncalieri (Torino), was built around 1960. It is in the proximity of a bridge with high traffic density. It showed the formation of a network of microcracks on the internal walls (both within the apartments and around the stairs), and the occurrence of wide cracks on the external walls. No significant cracks were detected in the concrete foundations nor in the concrete structure. Indeed, vibrations due to the heavy traffic are felt in the apartments at the top floors. In order to assess the stability of the structure, two column-beam joints located in the central part of the building, at the lower floor, were monitored (Fig. 7).

The structure has been continuously monitored for 40 days, corresponding to 960 h. During this period of time, a rehabilitation activity was carried out on the roof and on the facade of the building. Acoustic emissions have not been revealed during the stops of the intervention, whereas transducers perceived significant signals during the working days. Therefore, the AE analysis permits to assert that the structural behaviour is stable, since the AE activity was practically absent during normal situations (implying that no energy was released under service loads, i.e. damage was not propagating). In this specific case, the absence of AE activity shows that the traffic vibrations, although perceptible in the building, are efficiently absorbed by the structure damping capacity and do not result in cracking phenomena. On the other hand, the crack networks revealed on the vertical walls of the building can be ascribed to significant deformability and creep of the concrete floors.

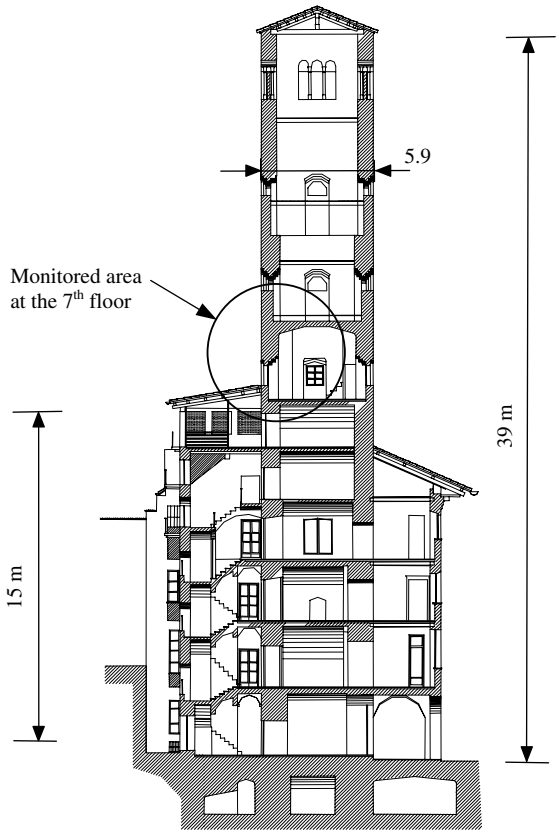

Fig. 5. Tower cross-section.

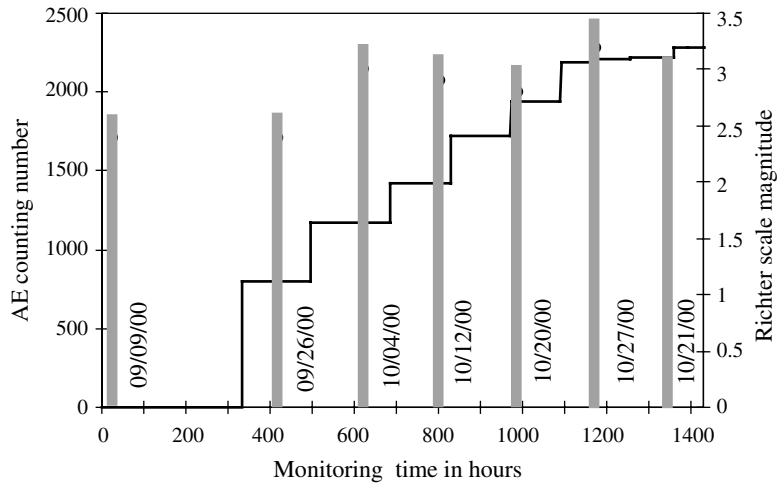

Fig. 6. Sineo Tower monitoring.

The second building that was monitored is located in Cascine Vica (Torino). In this case, four important macrocracks appeared on a concrete retaining wall situated at the bottom of the structure. Cracks started from the foundations of the wall and propagated vertically, extending throughout the width and stopping only against a steel-reinforced beam just below the concrete columns (Fig. 8).

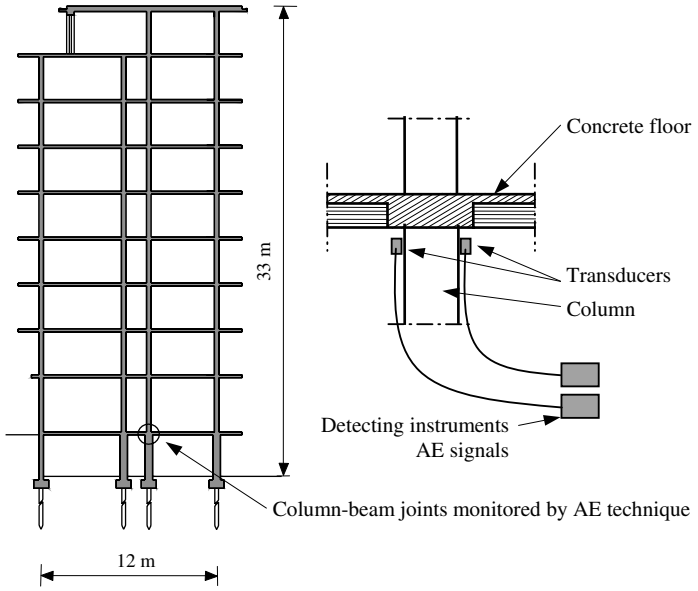

Fig. 7. Building in Moncalieri. Structural section of the building and location of transducers on column-beam joints.

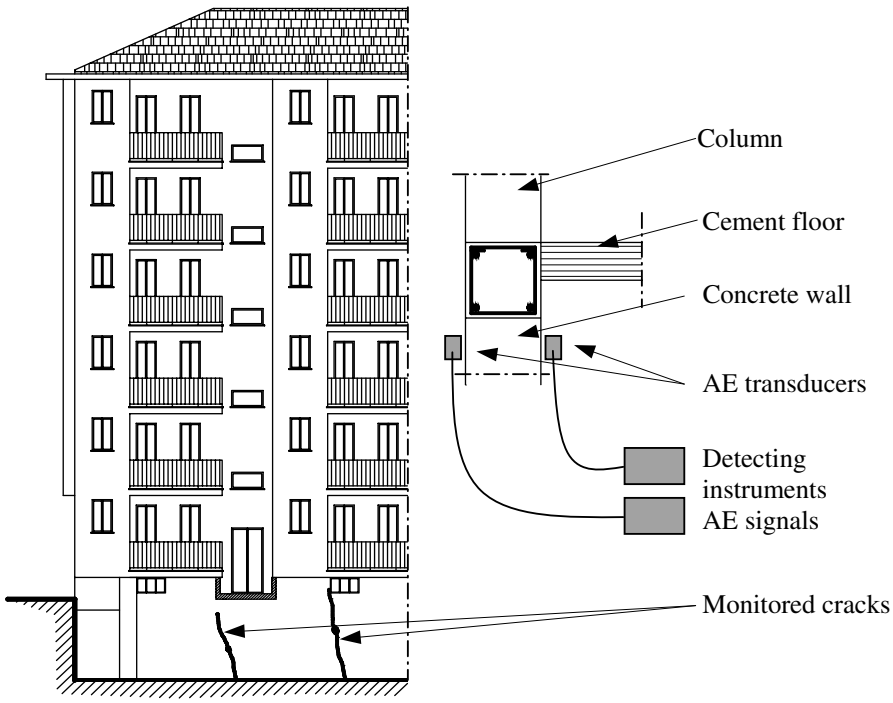

Fig. 8. Building in Cascine Vica. Cracking framework and location of transducers on the concrete wall.

The average crack opening was equal to 2 mm at the bottom and to almost 0.2 mm at the top of the wall. We have chosen to monitor two main cracks which had not already reached the upper beam. We tried to evaluate the propagation speed of these cracks and to predict their future development based on the cumulative AE count.

The advancement was monitored, in the case of both cracks, for almost 1000 h. The cumulative counts and the advancement of the crack are reported and compared in Fig. 9.

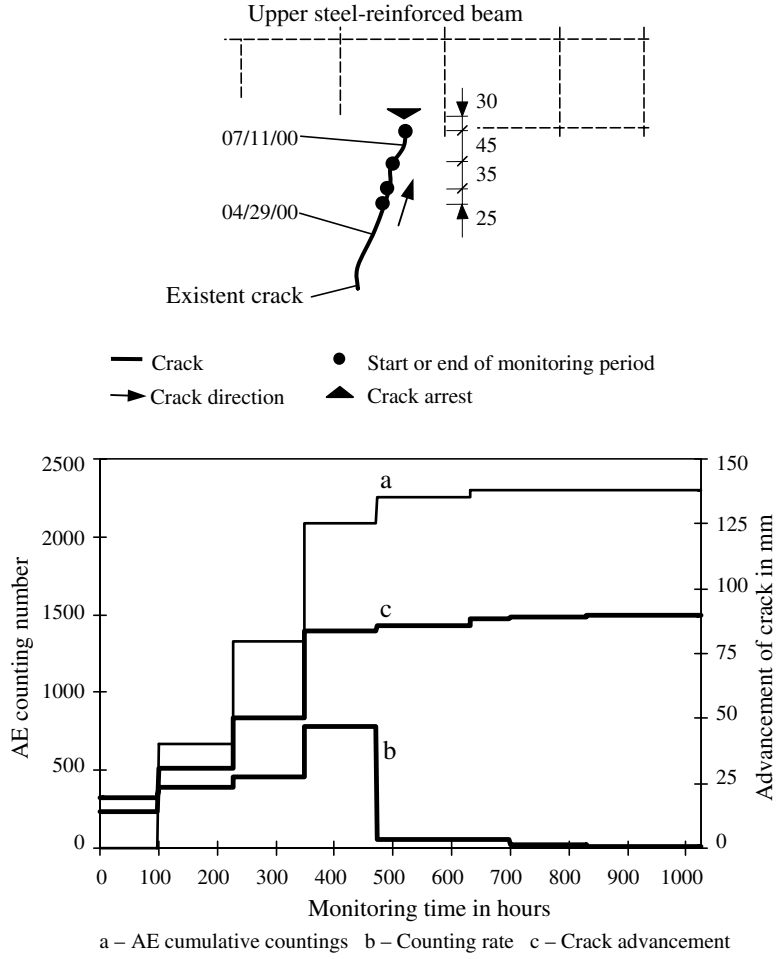

Fig. 9. Results of monitoring with AE technique.

Notice that, at any stage of the test, the oscillation count is proportional to crack propagation and that a reduction of AE density is directly related to crack arrest in the proximity of the upper beam (where a significantly larger toughness is attained due to steel reinforcement).

Since the highest number of AE counts detected during the test corresponds to the maximum velocity of crack propagation, we can deduce that the local maxima of the AE distribution function correspond to the most critical periods of propagation.

5. AE testing on a highway viaduct

By means of the AE technique we also analysed the damage evolution in two pilasters sustaining a viaduct along an Italian highway built in the 1950s (Fig. 10). From the pilasters we drilled some concrete cylindrical specimens in order to detect the mechanical properties of the material under compression and to evaluate the scale effects in size and time on AE activity [22].

5.1. Test specimens and testing equipment

The concrete, of good mechanical characteristics, presents an apparent specific weight of about 2.22 g/cm^3 and a maximum aggregate size of about 15 mm. For each pilaster, three different specimen diameters d are considered in a maximum scale range of 1:3.4. The specimens present three different slendernesses: $\lambda = h/d = 0.5$,

Fig. 10. The viaduct and the monitored pilasters P_1 and P_2 with the applied sensor.

1.0 and 2.0, with d chosen equal to 27.7, 59, 94 mm, respectively. For each of these nine geometries, three specimens have been tested, for a total of 54 cases (two pilasters). The geometries of some tested specimens are presented in Fig. 11. The average values obtained from the experimental data are reported in Table 1. The tests were performed by a MTS machine (810 model), which is controlled by an electronic closed-loop servo-hydraulic system (Fig. 12). It is therefore possible performing tests under load or displacement control. The displacements are recorded by a couple of inductive-bridge transducers (HBM W10 model) applied to the loading platens, with a maximum stroke of 10 mm.

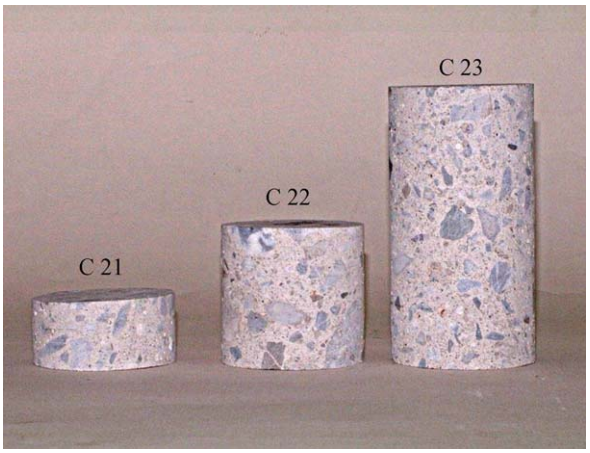

Fig. 11. Geometries of some tested specimens.

Table 1
Average values for the specimens obtained form pilasters P_1 and P_2

Specimen type	Diameter d [mm]	Slenderness $\lambda = h/d$	Pilaster P1			Pilaster P2		
			Peak stress σ_u [MPa]	N_{max} at σ_u	β_t	Peak stress σ_u [MPa]	N_{max} at σ_u	β_t
C11	27.7	0.5	91.9	1186	1.40	84.7	1180	1.38
C12	27.7	1.0	62.8	1191	1.41	46.7	1181	1.46
C13	27.7	2.0	48.1	1188	1.48	45.8	1186	1.67
C21	59.0	0.5	68.1	8936	2.12	57.5	8924	2.39
C22	59.0	1.0	53.1	8934	1.49	41.7	8930	2.52
C23	59.0	2.0	47.8	8903	2.30	38.2	8889	2.41
C31	94.0	0.5	61.3	28,502	2.90	45.2	28,484	2.84
C32	94.0	1.0	47.8	28,721	2.09	38.2	28,715	2.21
C33	94.0	2.0	44.1	28,965	2.80	38.1	28,956	2.92

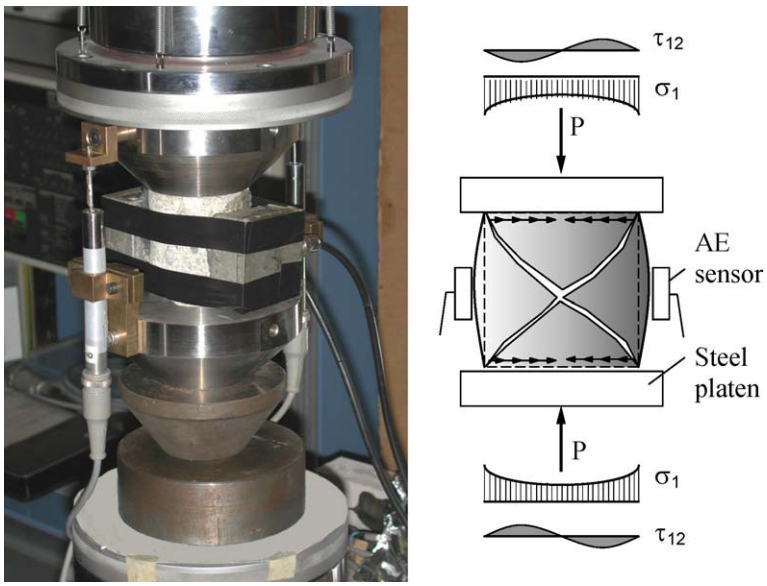

Fig. 12. Apparatus adopted for compression tests.

5.2. Displacement control and boundary conditions

All compression tests were performed under displacement control, by imposing a constant rate to the upper loading platen. We adopted a displacement rate equal to 10^{-4} mm/s for all specimens, in order to obtain a very slow-crack growth and to detect all possible AE signals. In this way, we were able to capture also the softening branch of the stress–strain diagrams.

The system adopted in the compression test utilizes rigid steel platens, the lateral deformation of concrete being therefore confined at the specimen ends, which are forced to have the same lateral deformation as the rigid platens. In this case, shear-stresses develop between specimen and loading platen, causing a three-dimensional state of stress at the specimen ends [23,24].

5.3. AE data acquisition system

The apparatus consists of two piezo-electric transducers (PZT), applied on the specimen surface and calibrated in the frequency range between 100 and 400 kHz, and of two data acquisition systems [11]. The threshold level of the signal is set equal to 100 μV and is amplified up to 100 mV. The oscillation counting capacity

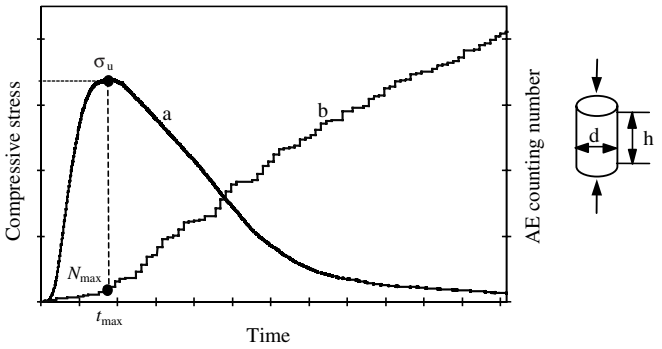

Fig. 13. Stress and cumulated event number versus time.

has been set equal to 255 counts per each period of 120 s, i.e. a single *event* is the result of 2 recording minutes. By means of this system, the intensity of a single event is by definition proportional to the number of counts N recorded in the time interval (Event-Counting). Clearly, this hypothesis is fully justified at the occurrence of slow-crack growth [25].

The stress and cumulated event number versus time for a specimen of intermediate size is represented in Fig. 13. In the figure the critical number of AE cumulative events $N_{\max}$ is represented in correspondence of the peak stress σ_u. Similar results can be observed in the other cases.

6. A fractal criterion for AE monitoring

A statistical and fractal analysis of laboratory experimental data was performed, considering the multiscale aspect of cracking phenomena. This approach shows that the energy dissipation, detected by AE, occurs in a fractal domain. Consequently, a multiscale criterion to predict the damage evolution and the time to structural collapse is formulated.

Recent developments in fragmentation theories [14–16] have shown that the energy dissipation E during microcrack propagation occurs in a fractal domain comprised between a surface and the specimen volume V. The result is that the total dissipated energy $E_{\max}$ after fragmentation scales as

$$E_{\max} = \Gamma V^{D/3}, \tag{1}$$

where Γ is the critical value of *fractal energy density* and D is the so-called fractal exponent, comprised between 2 and 3. As a consequence, the energy density scales as

$$\Psi = \frac{E_{\max}}{V} = \Gamma V^{(D-3)/3}. \tag{2}$$

This implies that not the energy density but the fractal energy density (having anomalous physical dimensions)

$$\Gamma = \frac{E_{\max}}{V^{D/3}}, \tag{3}$$

can be considered as a size-independent parameter.

On the other hand, during microcrack propagation, acoustic emissions can be clearly detected. The dissipated energy E is proportional to the number N of acoustic emission events (with intensity proportional to $\Delta N/\Delta t$, where t is the time). Accordingly to the energy dissipation over a fractal domain—as described by Eq. (3)—the critical number of acoustic emissions $N_{\max}$, not over a volume but over a fractal domain, can be considered as a size-independent parameter:

$$\Gamma_{\mathrm{AE}} = \frac{N_{\max}}{V^{D/3}}, \tag{4}$$

where Γ_{AE} is the critical value of *fractal acoustic emission density*.

The fractal criterion (4) predicts a *volume-effect* on the maximum number of acoustic emission events, that, in a bilogarithmic diagram, would appear as

$$\log N_{\max} = \log \Gamma_{\mathrm{AE}} + \frac{D}{3} \log V \tag{5}$$

with a slope equal to $D/3$.

6.1. Damage level

The damage level of a structure can be obtained from AE data of a reference specimen (pedex r) extracted from the structure and tested up to rupture. From Eq. (4) we have:

$$N_{\max} = N_{\max\, r} \left(\frac{V}{V_r} \right)^{D/3}, \tag{6}$$

from which we can obtain the critical number of acoustic emission events $N_{\max}$ that the structure may provide before achieving the collapse. Naturally, the underlying assumption is that the damage level observed in the reference specimen is proportional to the level reached in the entire structure before monitoring is started. An energy parameter describing the damage level of the structure during the monitoring process can be defined as the following ratio:

$$\eta = \frac{E}{E_{\max}} = \frac{N}{N_{\max}}, \tag{7}$$

N being the cumulative AE events number obtained during monitoring.

6.2. Size effects

Considering geometrical self-similar structures of characteristic size ℓ, i.e. $V \cong \ell^3$, Eq. (5) becomes:

$$\log N_{\max} = \log \Gamma_{\mathrm{AE}} + D \log \ell, \tag{8}$$

predicting a size effect on AE.

6.3. Shape effects

Considering specimens with the same base side d and different slenderness λ, i.e. $V \cong \lambda d^3$, Eq. (5) becomes:

$$\log N_{\max} = \log(\Gamma_{\mathrm{AE}} d^D) + \frac{D}{3} \log \lambda, \tag{9}$$

predicting a shape effect on AE.

6.4. Time dependence on AE

The damage level of Eq. (7) can be also expressed as a function of time t:

$$\eta = \left(\frac{t}{t_{\max}} \right)^{\beta_t}, \tag{10}$$

where the exponent β_t can be obtained from the AE data of a reference specimen. The β_t values plotted versus the specimen diameters are reported in Fig. 14. The observed trend is an increase of the β_t values by increasing the specimen diameter (Table 1). The experimental time-scaling agrees with the fractal law of Eq. (10), giving an exponent in the range $(0, 3)$ [26]. The damage level parameter being known, from Eq. (10) we can evaluate the life-time $t_{\max}$ of the structure monitored for a time period t.

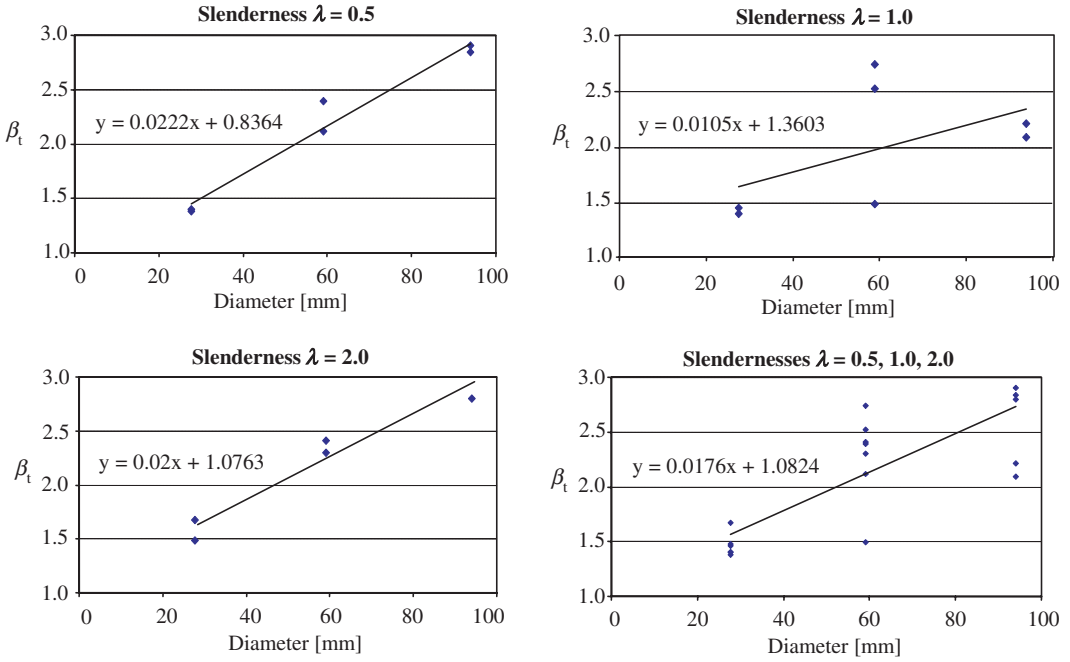

Fig. 14. Life-time exponent β_t plotted versus specimens diameter.

6.5. Comments on the results entered in Table 1

The dependence of concrete properties on the loading system and specimen geometry is an important question in understanding the deformation and failure behaviour of concrete under loading. Although experimental studies are numerous, theoretical studies on concrete specimens regarding the parametrical analysis of loading platens on strength characterization, the amount of energy dissipated and pre- and post-peak behaviour are rare [23,24].

Based on the laboratory tests conducted during this investigation up to peak stress, as summarised in Table 1, the following considerations can be made. Concrete strength and the evolution of stress–strain curves in compression is affected first of all by factors associated with concrete mix-design; secondly, if a specimen is already damaged, the quantity of pre-existing internal bond cracks also comes into play. For this reason, if we compare the strength values of specimens of the same size belonging to the two pilasters, we shall find that the values of peak stress for pilaster P_2 are about 10% lower than those for pilaster P_1.

Other major aspects affecting concrete failure in compression include: *type of contact*, depending on the platens utilized; the *shape of the element*, defined in terms of the ratio between specimen height h and the characteristic size of specimen cross-section d; the characteristic *element size scale* d. As for the effects due to end constraints, friction, caused by stiff steel platens, affects the stress field, inducing radial compressive stresses close to the ends; the higher is the h/d ratio, the faster these effects vanish far from the ends. As a rule, these phenomena become more noticeable in the post-peak stage and entail the transition from crushing to splitting for uniaxially compressed specimens. On the other hand, a different situation would emerge for softer loading platens, equipped, for example, with a thin layer of Teflon in contact between the platen and the specimen. In this case, the platens would cause a large lateral deformation, giving rise to outward-directed shear forces at the interface. When the factional forces are directed outward, a biaxial tension/compression state of stress develops in the specimen ends and a splitting type of failure is often seen to occur.

As can be seen from Table 1, the pre-peak portion of the stress–strain curves shows that specimen size and slenderness have significant effects on peak stresses σ_u. This result, based on experimental findings, is explained by linear elastic fracture mechanics [23,24]. However, it has also been ascertained that a change in specimen size does not have appreciable effects on damage patterns [27]. Highly significant are the size effects on the

critical number of acoustic emission N_{max}, but the same parameter N_{max} is seen to be less sensitive to slenderness. This is due to the fact that failure of concrete in uniaxial compression is caused by the localization of damage in a zone of finite dimensions, and damage only begins to localize close to the peak load. Fractured areas are more deformed while unfractured portions recover their deformations. When critical conditions are reached, specimens with greater slenderness are characterised by a smaller damaged volume compared to lower slenderness specimens. The confinement induced by stiff platens increases the strength of the specimens but causes material fragmentation only near the bases.

Hence, the effects of slenderness on parameter N_{max} are not noticeable, as the released energy measured by the AE technique is correlated to the area subtended by the stress–strain curve. This area is correlated to the ductility of the material, which, as a rule, is not proportional to its strength. For these reasons, when monitoring full scale structures, it is reasonable to make predictions on the maximum number of AEs that would lead to the critical stage, by taking into account total volume damaged. An example is given in the next section.

7. Experimental assessment and lifetime prediction

A comparison between experimental results and theoretical predictions is herein presented. For all the tested specimens, the critical number of acoustic emissions N_{max} was evaluated in correspondence to the peak-stress σ_u.

On average compression tests show an increase in AE cumulative event number by increasing the specimen volume. Subjecting the average experimental data to a statistical analysis (Table 1), we can quantify the parameters D and Γ_{AE} in Eq. (5). The parameter D represents the slope, in the bilogarithmic diagram, of the curve that relates N_{max} to the specimen volume. From the best-fitting, we obtain $D/3 \cong 0.766$ (Fig. 15), so that the fractal exponent results, as predicted by the fragmentation theories, to be comprised between 2 and 3 ($D \cong 2.3$). Moreover, the critical value of fractal acoustic emission density results to be: $\Gamma_{AE} \cong 170\ \mathrm{cm}^{-2.3}$.

An example of the N/N_{max} versus time dependence is given in Fig. 16. After an initial transient period ($0 < t/t_{max} < 0.4$), a true power-law scaling is observed [28]. From the best-fitting in the bilogarithmic plane (Fig. 15), for the tested specimen, having average properties, C22 ($d = 59$ mm, $\lambda = 1$) we obtain the slope $\beta_t = 2.52$, as reported in Eq. (10). Similar results can be observed for stress and strain dependencies. For the same specimen, the damage time evolution is also represented (Fig. 16b), fitted to experimental data.

The two pilasters, mentioned in the Section 5, were monitored utilizing the described AE data acquisition system. During the observation period (172 days), we obtained a number of events $N \cong 2 \times 10^5$ for the more damaged pilaster P_1, and $N \cong 8 \times 10^4$ for the less damaged P_2, respectively. Since the volume of each pilaster is

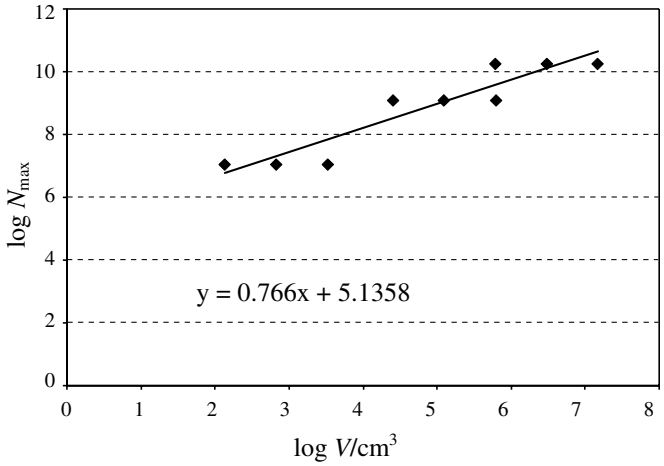

Fig. 15. Volume-effect on N_{max}.

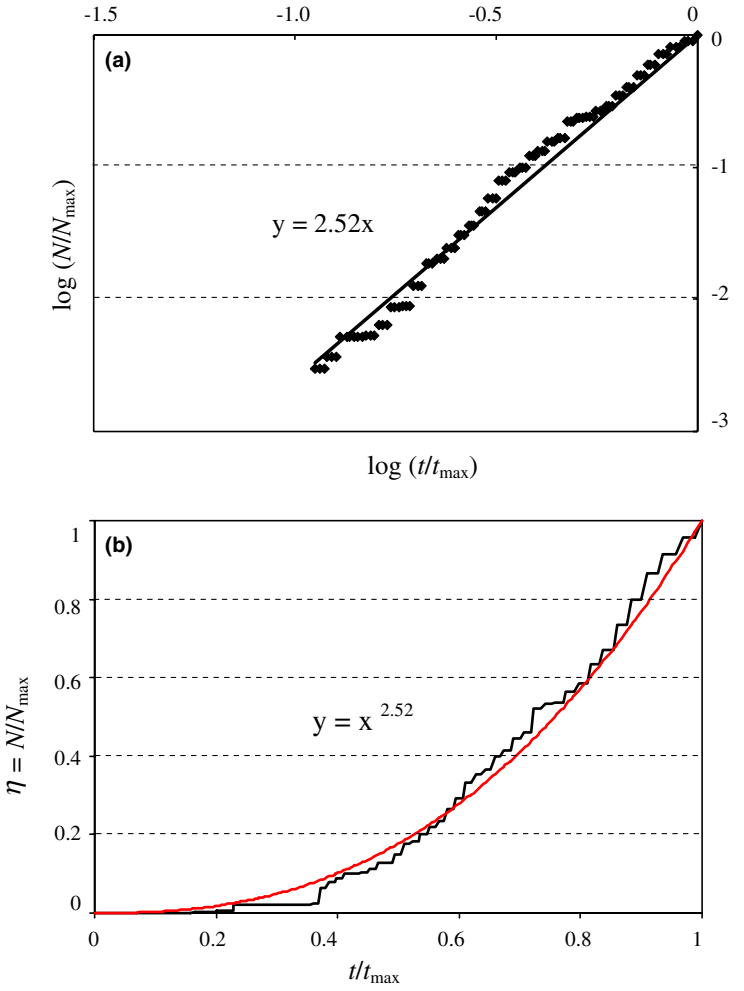

Fig. 16. Damage evolution.

about 2×10^6 cm^3, from Eq. (5), utilizing the fractal exponent $D \cong 2.3$ and a fractal acoustic emission density $\Gamma_{AE} \cong 170\ \text{cm}^{-2.3}$, we obtain the critical number of AE equal to $N_{max} \cong 11.51 \times 10^6$.

Inserting the values of N and N_{max} into Eq. (9), and assuming an exponent $\beta_t = 2.52$ of Fig. 16 (a more conservative choice would be 3), we obtain $t/t_{max} \cong 0.2$ for pilaster P_1, and $t/t_{max} \cong 0.14$ for pilaster P_2. The lifetime of these structural elements is therefore defined, corresponding to the achievement of the maximum number of events, at, respectively, 2.4 and 3.4 years, considering the time origin from the instant in which the specimens have been drilled.

8. Conclusions

In the first part of this work we have meant to describe the application of the AE technique to monitor concrete and masonry buildings. In particular we have proposed an innovative methodology, based on the counting of events, in order to determine the released energy and therefore the conditions of stability or the risk due to the spreading of discrete cracks.

In the second part, the interpretation is presented of quasi-brittle material behaviour in compression, utilizing the AE technique and based on statistical and fractal analysis. Such an approach has shown that the energy dissipation caused by diffused damaging, such as is produced by compression, measured by the number of acoustic emissions N, occurs over a fractal domain.

The laboratory experiments, performed on concrete specimens of different size and slenderness, show size-effects characterized by fractal exponents according to the fragmentation theories. By varying the slenderness, no shape effects are observed. This means that, during the compression tests, friction between loading platens and specimen produces the material fragmentation only near the bases. Therefore, the fragmented volume releasing AE results to be independent of the slenderness. Eventually, a multiscale criterion to predict the damage evolution, also in large concrete structural elements, was formulated.

By monitoring the evolution of damage by means of the AE technique, it is therefore possible to evaluate the damage level as well as the time to final collapse for structures subject to diffused damaged as is caused by compression. Or it is possible to ascertain stability or instability conditions and to forecast the extent of damage in structures characterised by the propagation of discrete cracks.

Acknowledgements

The present research was carried out with the financial support of the Ministry of University and Scientific Research (MIUR) and of the European Union (EU).

The authors like to thank the Architects Massimo Aprile and Luigi Bacco for the technical support provided in the structural monitoring.

References

[1] Carpinteri A, Bocca P. Damage and diagnosis of materials and structures. Bologna: Pitagora Editrice; 1991.
[2] Ohtsu M. The history and development of acoustic emission in concrete engineering. Mag Concr Res 1996;48:321–30.
[3] Kaiser J. An investigation into the occurrence of noises in tensile tests, or a study of acoustic phenomena in tensile tests. PhD dissertation, Technische Hochschule Münschen, Munich FR, 1950.
[4] Rüsch H. Physical problems in the testing of concrete. Zem-Kalk-Gips (Wiesbaden) 1959;12:1–9.
[5] L'Hermite RG. Volume change of concrete. In: Proc 4th int symp on chemistry of cement, V-3. NBS monograph 43, NBS, Washington, DC, 1960. p. 659–94.
[6] Robinson GS. Methods of detecting the formation and propagation of microcracks in concrete. In: Proc int conf on the structure of concrete and its behavior under load. Cement and Concrete Association, 1965. p. 131–45.
[7] McCabe WM, Koerner RM, Load Jr AE. Acoustic emission behavior of concrete laboratory specimens. ACI J 1976;13:367–71.
[8] Niwa Y, Kobayashi S, Ohtsu M. Studies of AE in concrete structures. Proc JSCE 1978;276:135–47.
[9] Shah P, Li Z. Localization of microcracking in concrete under uniaxial tension. ACI Mater J 1994;91:372–81.
[10] Carpinteri A, Lacidogna G. Monitoring a masonry building of the 18th century by the acoustic emission technique. In: Proc of STREMAH VII, Bologna, 2001. Southampton: WIT Press; 2001. p. 327–37.
[11] Carpinteri A, Lacidogna G. Structural monitoring and diagnostics by the acoustic emission technique: scaling of dissipated energy in compression. In: Proc of the 9th int cong, on sound and vibration (ICSV9), Orlando, FL, USA, 2002. Paper No. 166.
[12] Carpinteri A, Lacidogna G. Damage diagnosis in concrete and masonry structures by acoustic emission technique. J Facta Univ 2003; 3:755–64.
[13] Carpinteri A, Lacidogna G, Pugno N. Acoustic emission during fragmentation of quasi-brittle materials in compression. In: Proc of 16th AIMETA cong, of theoretical and applied mechanics, Ferrara, Italy, 2003. Paper No. 119.
[14] Carpinteri A, Pugno N. Fractal fragmentation theory for shape effects of quasi-brittle materials in compression. Mag Concr Res 2002; 54:473–80.
[15] Carpinteri A, Pugno N. A fractal comminution approach to evaluate the drilling energy dissipation. Int J Numer Anal Meth Geomech 2002;26:499–513.
[16] Carpinteri A, Pugno N. A multifractal comminution approach for drilling scaling laws. Powder Technol 2003;131:93–8.
[17] Richter CF. Elementary seismology. San Francisco and London: WH Freeman and Company; 1958.
[18] Chakrabarti BK, Benguigui LG. Statistical physics of fracture and breakdown in disordered systems. Oxford: Clarendon Press; 1997.
[19] Pollock AA. Acoustic emission-2: acoustic emission amplitudes. Non-Destruct Test 1973;6:264–9.
[20] Brindley BJ, Holt J, Palmer IG. Acoustic emission-3: the use of ring-down counting. Non-Destruct Test 1973;6:299–306.
[21] Carpinteri A, Chiaia B, Lacidogna G. Onset of catastrophic failure in concrete frames: safety assessment by acoustic emission. In: Proc of the int FIB conference concrete structures in the 21st century, Osaka, 2002. p. 55–62.
[22] Carpinteri A, Lacidogna G, Pugno N. Damage diagnosis and life-time assessment of concrete and masonry structures by an acoustic emission technique. In: Li VC, Leung CKY, Willam KJ, Billington SL, editors. Proc of 5th int conf on fracture mechanics of concrete and concrete structures (FraMCos-5), Vail, Colorado-USA, 2004. p. 31–40.
[23] Carpinteri A, Ferro G, Monetto I. Scale effects in uniaxially compressed concrete specimens. Mag Concr Res 1999;51:217–25.
[24] Carpinteri A, Ciola F, Pugno N. Boundary element method for the strain-softening response of quasi-brittle materials in compression. Comput Struct 2001;79:389–401.

[25] Holroyd T. The acoustic emission and ultrasonic monitoring handbook. Oxford: Coxmoor Publishing Company's; 2000.
[26] Carpinteri A, Lacidogna G, Pugno N. Time effects on acoustic emission due to elastic waves propagation in monitored cracking solids. In: Proc of 11th int conf on fracture (ICF11), Torino, Italy, 2005.
[27] Carpinteri A, Lacidogna G, Pugno N. Scaling of energy dissipation in crushing and fragmentation: a fractal and statistical analysis based on particle size distribution. Int J Fract 2004;129:131–9.
[28] Shcherbakov R, Turcotte DL. Damage and self-similarity in fracture. Theor Appl Fract Mech 2003;39:245–58.